Improving ovarian cancer treatment decision using a novel risk predictive tool

Zhenyi Xu[1,*], Jiali Song[2,*], Lei Cao[1], Zhiwei Rong[2], Wenjie Zhang[1], Jia He[1], Kang Li[1], Yan Hou[2]

[1]Department of Epidemiology and Biostatistics, School of Public Health, Harbin Medical University, Harbin 150086, China
[2]Department of Biostatistics, Peking University, Beijing 100000, China
[*]Equal contribution as first authors

Correspondence to: Kang Li, Yan Hou; **email:** likang@ems.hrbmu.edu.cn, houyan@bjmu.edu.cn

ABSTRACT

Background: As a major component of the tumor tissue, the tumor microenvironment (TME) has been proven to associate with tumor progression and immunotherapy. Ovarian cancer accounts for the highest mortality rate among gynecologic malignances. Its clinical treatment decision is highly correlated with the prognosis, underscoring the need to evaluate the prognosis and choose the proper clinical treatment through TME information.

Method: This study constructs a score with TME information obtained by the CIBERSORT algorithm, which classifies the patients into high and low TMEscore groups with quantified TME infiltration patterns through the PCA algorithm. TMEscore was constructed by TCGA cohort and validated in GEO cohort. Univariate and multivariate Cox proportional hazards model analyses were used to demonstrate prognostic value of TMEscore in overall and stratified analysis.

Result: TMEscore is highly correlated with survival and high TMEscore group has a better prognosis. In order to improve treatment decision, the expression of immune checkpoints, immunophenoscore (IPS) and ESTIMATE score showed a high TMEscore have a better immune microenvironment and respond better to immune checkpoint inhibitors (ICIs). Meanwhile, the mutation landscape between TMEscore groups was profiled, and 13 genes were found mutated differently between the two groups. Among them, BRCA1 has more mutations in the high TMEscore group and speculated that high TMEscore patients might be a beneficiary population of PARP inhibitors combined with immunotherapy.

Conclusion: TMEscore based on TME with prognostic value and clinical value is proposed for the identification of targets treatment and immunotherapy strategies for ovarian cancer.

INTRODUCTION

The tumor microenvironment (TME) is created by the tumor and dominated by tumor-induced interactions [1]. Within the TME infrastructure, various types of immune (innate and adaptive immune cells) and non-immune (stromal cells, fibroblasts, endothelial cells) are found. These cells drive a chronic inflammatory, immunosuppressive, and pro-angiogenic intratumoral

environment by secreting downstream factors [2, 3]. To date, several studies have found that TME not only plays an essential role in tumor initiation, disease progression, and metastatic development but also has profound effects on therapeutic efficacy [4]. Therefore, identifying effective targeted drugs with TME provides new insights into case-specific medical care. Immune checkpoints such as programmed death (PD-1) and its ligand (PD-1 ligand [PD-L1]) have been found ligand-

receptor interactions between cancer cells and host immune cells in TME. The corresponding monoclonal antibody agents like nivolumab and pembrolizumab have been approved by the Food and Drug Administration (FDA) to treat melanoma, lung, gastric cancer, etc. [5, 6]. Even though these drugs could prolong overall survival (OS) and progression-free survival (PFS), still only a small subset of patients benefit from these drugs [7, 8]. Therefore, it is vital to accurately identify prognostic biomarkers and the therapeutic beneficiaries in future research directions.

Ovarian cancer is the leading cause of death among patients with gynecologic malignancies [9]. About 80% of patients with serious carcinomas are diagnosed at an advanced stage [10]. Even though more than 80% of patients with advanced-stage respond to cytoreductive surgery and adjuvant chemotherapies, most of them ultimately relapse and eventually develop chemotherapy-resistant disease [11]. Recently, PARP inhibitors and Bevacizumab have been approved for ovarian cancer in addition to platinum-based therapies [12]. Immunotherapy presents a potentially novel frontier in ovarian cancer treatment, but the response rates among ovarian cancer patients is not quite high as expected. A phase II study of nivolumab (anti–PD-1 antibody) monotherapy found a 15% overall response rate (ORR) in 20 patients with platinum-resistant disease, while another combination therapy with nivolumab and bevacizumab show a 40% ORR in 38 patients with relapsed ovarian cancer in platinum-sensitive patients and 16.7% in platinum-resistant patients [7, 13]. It is evident that not all patients can benefit from immunotherapy, and patients sensitive to first-line platinum-based therapy had a higher response rate to immunotherapy than platinum-resistant patients.

This paper aims to construct a prognostic biomarker with TME and predict therapeutic effects. At present, the prognostic models consist of the commonly used prognostic indicators, such as clinicopathological characteristics and various biomarkers. However, the interaction between genes and the bias of gene expression values across platforms may lead to differences across studies. In this study, we started by systematically characterizing TME in ovarian cancer using CIBERSORT computational algorithms [14]. Then, the score with quantified TME infiltration pattern (namely TMEscore) through Principal Components Analysis (PCA) algorithm was constructed and systematically correlated with platinum-based therapy and clinical features in ovarian cancer. Finally, we explored the response to ICIs in different TMEscore groups and the association between TMEscore and mutation landscape to identify potential targets and feasible treatments.

RESULTS

Landscape of TME cells in ovarian cancer

The workflow for this study is shown in Supplementary Figure 1. The landscape with LM22 in TCGA was analyzed by CIBERSORT computational algorithms (Supplementary Table 1). With the NMF method, cluster numbers $k = 3$ was chosen as a final cluster number because of the suitability of clustering (Figure 1A) [15]. Finally, 373 samples with TME cell expression profiles were divided into three subgroups, named TME cluster-1, TME cluster-2 and TME cluster-3. We found that TME cluster-2 had a significantly longer OS than others ($P = 0.0102$; Figure 1B). TME cluster-2 exhibited high infiltration of CD8 T cells, activated memory CD4 T cells, follicular helper T cells, M1 macrophages, gamma delta T cells and so forth. While TME cluster-1 and TME cluster-3 were characterized by increases in the infiltration of resting mast cells, resting NK cells and M0 macrophages or M2 macrophages, activated dendritic cells, neutrophils and activated mast cells, respectively (Figure 1C).

TME signature and functional annotation

We identify 1,351 TME-related DEGs, which might be associated with the biological behavior of TME. Consensus clustering was used to unsupervised learning clusters of genes (Figure 2A–2D). According to heatmap of the consensus matrices, consensus cumulative distribution function (CDF) curve, two gene clusters, termed as gene-cluster A and gene-cluster B, were identified. The functions and pathways associated with the DEGs were analyzed using KEGG and GO. The gene-cluster A enriched in Cytokine-cytokine receptor interaction pathway, Chemokine signaling pathway, Viral protein interaction with cytokine and cytokine receptor pathway and so on. In contrast, gene-cluster B enriched in Focal adhesion pathway, PI3K-Akt signaling pathway, MAPK signaling pathway, Proteoglycans in cancer pathway etc. GO enrichment (biological process) showed that gene-cluster A mainly involved T cell activation, leukocyte cell-cell adhesion and leukocyte migration; gene-cluster B were significantly enriched in axonogenesis and regulation of protein-containing complex assembly. (Figure 2E, 2F, Supplementary Tables 2, 3). And top 100 DEGs were shown in Figure 2G.

Establishment of the TMEscore in TCGA database

The TMEscore was defined as $\text{TMEscore} = \sum PC1_i - \sum PC1_j$. The 373 patients in the TCGA cohort were divided into high or low TMEscore groups based on the TMEscore cutoff value (0.83). The

patients with low TMEscore had a worse prognosis in univariate analysis (HR, 1.818; 95% CI, 1.303–2.536; $P < 0.001$; Figure 3A). Adjusting for age, grade, stage and chemotherapy outcome, TMEscore (HR, 1.643; 95% CI, 1.118–2.413; $P = 0.011$) was an independent predictive factor of ovarian cancer, and its C-index was 0.688 ± 0.024 (Figure 3E). Furthermore, in subgroup analysis, we found that the TMEscore was still an independent predictive factor for patients with complete response (CR) of platinum drug chemotherapy, while TMEscore could not be identified as an independent predictive factor for non-CR (non-CR: partial response, progressive and stable disease) patients (Figure 3B, 3C and 3F, 3G). In addition, we combined CR and PR as the responders (CR and PR) and the others as the non-responders (non-CR and non-PR) and found that TMEscore could be used as an independent predictive factor in responders but not in non-responders
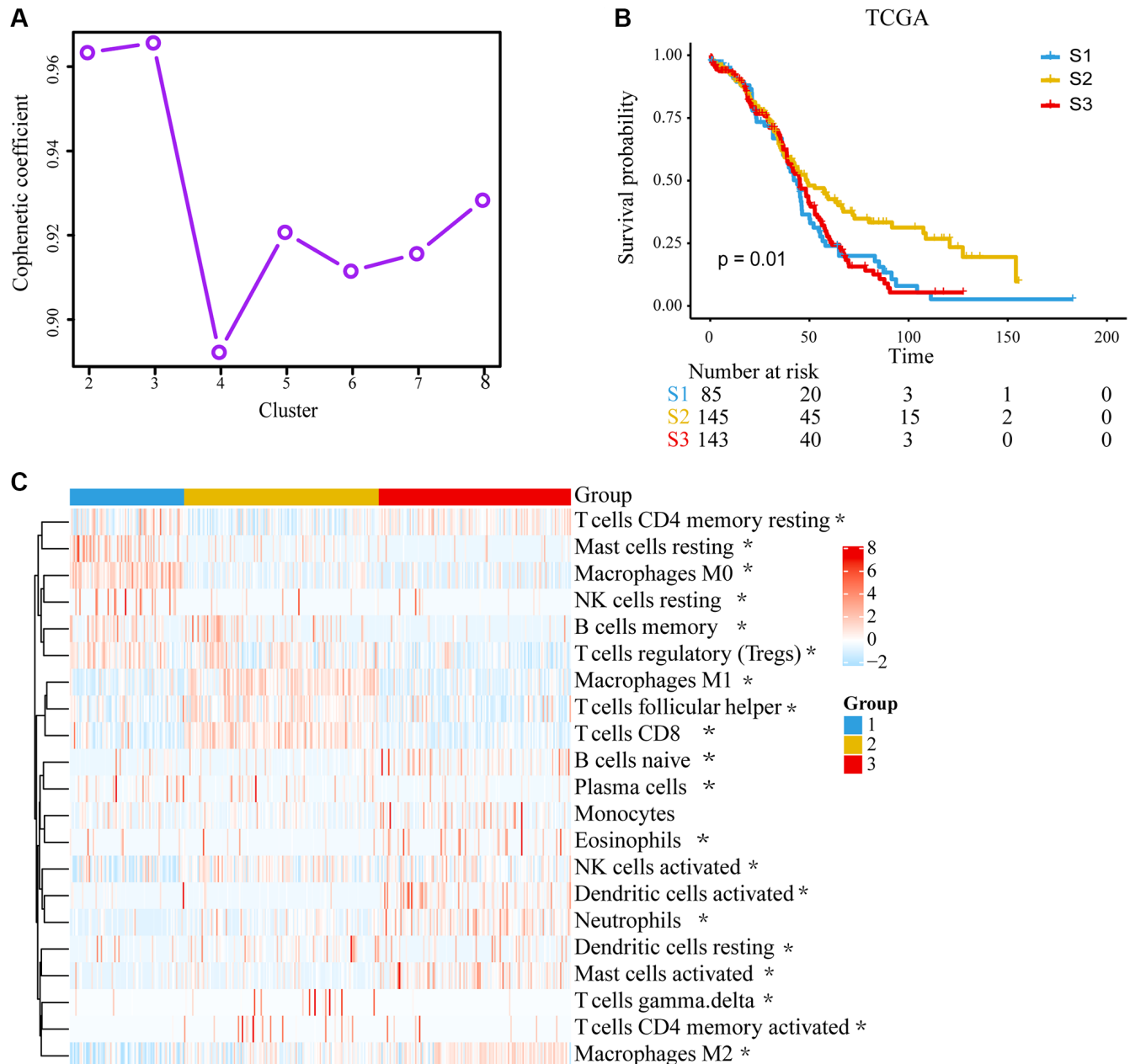

Figure 1. Unsupervised clustering of tumor microenvironment (TME) cells and subtype characteristics for 373 ovarian cancer patients in the TCGA cohort. (A) Cophenetic correlation coefficient of different clusters. (B) Kaplan–Meier (K–M) curves for overall survival (OS) of different 3 subtypes (log-rank test, $P = 0.010$). (C) Expression pattern of 21 TME cell types in 3 TME subtypes. The differences were confirmed by Kruskal–Wallis tests in the three TME subgroups with TME cell infiltration, and they were statistically significant except Monocytes. The asterisks represented the statistical P value. ($^{*}P < 0.05$).

(Supplementary Figure 2). Compared with the high TMEscore group, only a small number of DEGs in high TMEscore group were highly expressed in gene-cluster A. Meanwhile, high TMEscore group was concentrated on the CR, TME clusters-2, which were all related with better survival (Figure 3D).

Validation of the TMEscore in GEO database

We used independent datasets from the GEO database to further validate TMEscore. A total of 2,005 ovarian cancer patients were divided into high and low TMEscore groups by the same cutoff value. It was
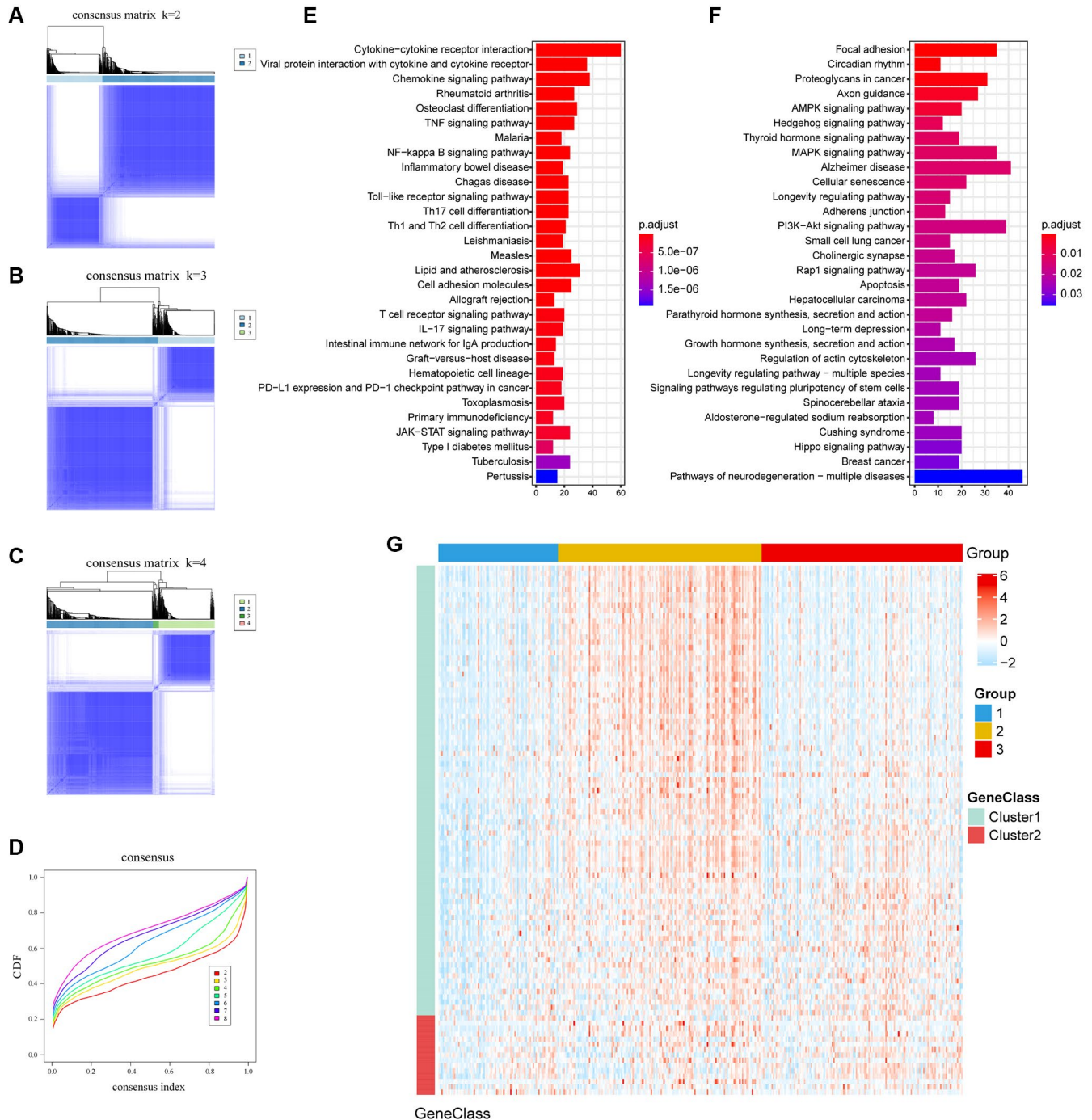

Figure 2. The clusters of DEGs with consensus clustering algorithm and KEGG enrichment. (**A–C**) Consensus matrixes of TCGA cohorts for each k (k = 2–4), displaying the clustering stability using 1000 iterations of hierarchical clustering. (**D**) Cumulative distribution function (CDF) curve; Different colors represent different clusters, x-axis denotes consensus index and y-axis denotes CDF values. (**E**, **F**) Enrichment pathways of the top 30 KEGG in gene cluster A and gene cluster B. (**G**) Expression profile heatmap of top 100 DEGs obtained by LIMMA and Random Forest.

found that low TMEscore group had a worse prognosis (HR, 1.275; 95% CI, 1.116–1.457; *P* < 0.001; Figure 4A). A multivariate Cox regression model was constructed, and its C-index was 0.677 ± 0.030, in which TMEscore (HR, 1.731; 95% CI, 0.997–3.005; *P* = 0.051) was might an independent prognostic factor (Figure 4E). Expression profile of DEGs was similar to TCGA and shown in Figure 4D. Further, in subgroup analysis, we found that TMEscore had a better performance to predict the prognosis for patients who showed CR than non-CR to chemotherapy (Figure 4B, 4C and 4F, 4G).

Consistent with TCGA, we redefined the chemotherapy outcome (CR and PR as responder; non-CR and non-PR as non-responder) and found TMEscore could be used as an independent predictive factor in responders (Supplementary Figure 3).

Establish a nomogram to predict the OS of ovarian cancer

To predict mortality in ovarian cancer patients, a nomogram was drawn in the TCGA dataset to serve as a clinically relevant quantitative method and age, stage,
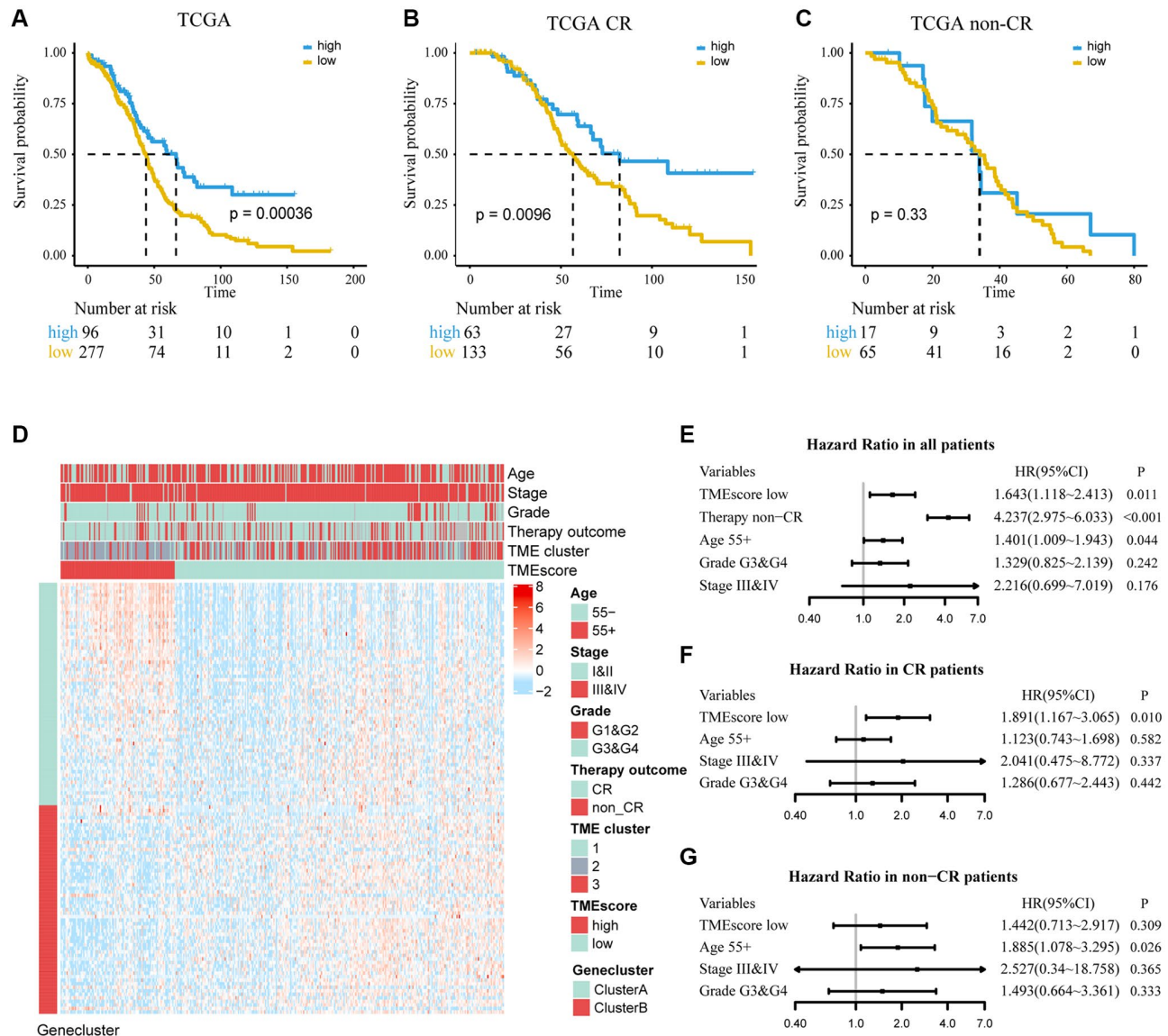

Figure 3. Determine the prognostic group of 373 ovarian cancer patients based on TMEscore in TCGA and evaluate the predictive ability. (**A**) K–M curve for OS of different TMEscore groups (log-rank test, *P* < 0.001). (**B**, **C**) According to chemotherapy outcome-stratified analysis (278 ovarian cancer patients), K–M curves in patients with complete response (CR) or non-complete response (non-CR) in different TMEscore group (log-rank test, *P* = 0.001; log-rank test, *P* = 0.33). (**D**) Expression profile of DEGs with survival significance. TMEscore, age, stage, grade, therapy outcome and TME cluster are shown as patient annotations. GeneClass is shown as gene annotations. Top legend, gray indicates missing value. (**E**–**G**) Forest plots illustrate the results of multivariate Cox proportional hazards model of clinical feature in all patients, CR patients and non-CR patients respectively.

grade and chemotherapy outcome were included respectively (Supplementary Figure 4A). Furthermore, calibration curves showed that the nomogram had similar performance to an ideal model, which could predict ovarian cancer survival at 3 and 5 years in a relatively stable manner (Supplementary Figure 4B, 4C). Due to the incomplete information on clinical features in the GEO dataset, we cannot further verify the nomogram in the GEO.

Profile tumor somatic mutation between TMEscore groups

To comprehensively understand and explore the appropriate treatment strategy for high and low TMEscore groups, the top 30 highly mutated genes distribution were shown in Supplementary Figure 5A, 5B. The mutation rate of TP53 was the highest, reaching 87% and 92% in high and low TMEscore
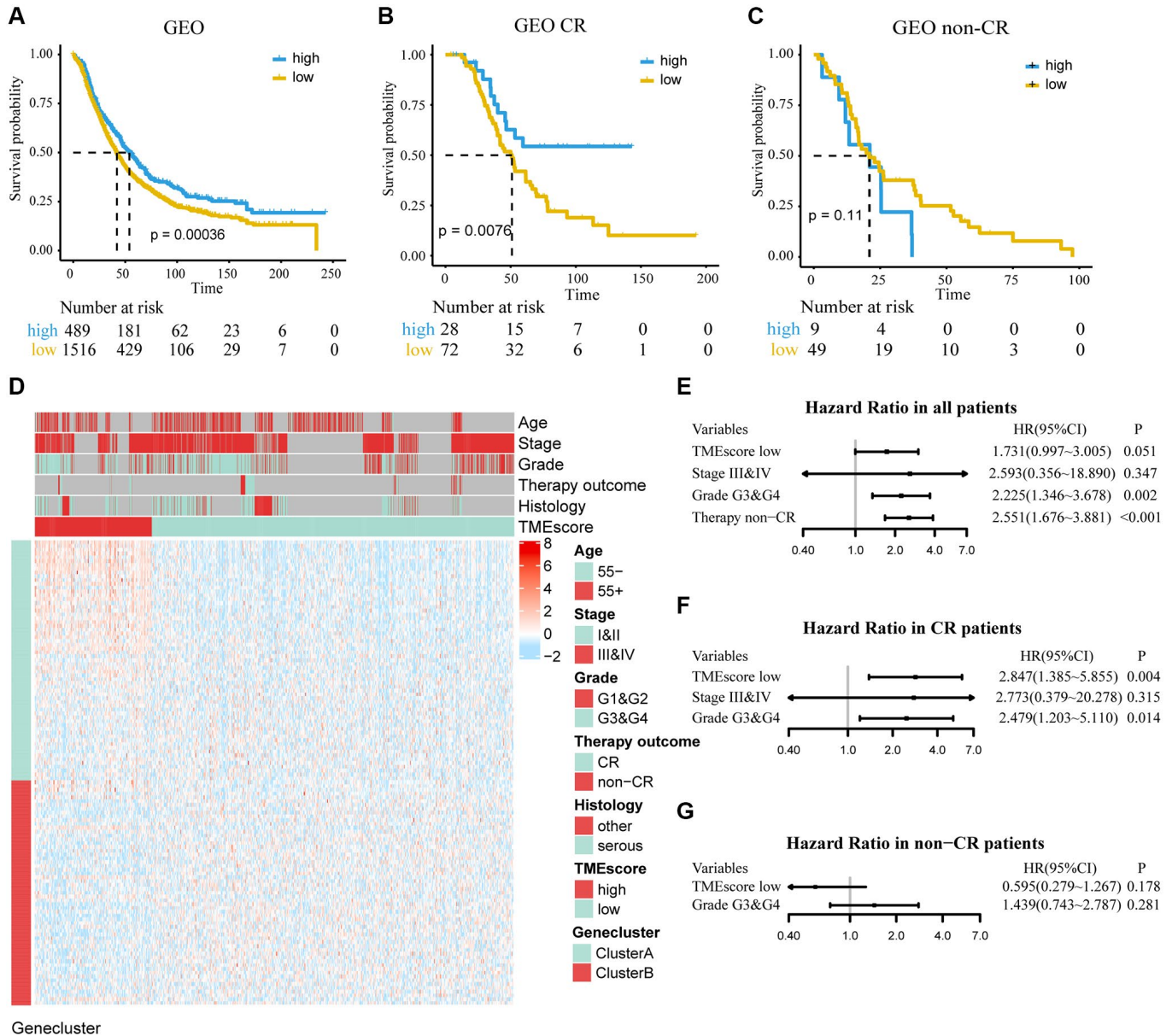

Figure 4. Determine the prognostic group of 2005 ovarian cancer patients based on TMEscore in GEO and evaluate the predictive ability. (**A**) K–M curve for OS of different TMEscore groups (log-rank test, *P* < 0.001). (**B**, **C**) According to chemotherapy outcome-stratified analysis (158 ovarian cancer patients), K–M curves in patients with complete response (CR) or non-complete response (non-CR) in different TMEscore group (log-rank test, *P* = 0.008; log-rank test, *P* = 0.11). (**D**) Expression profile of DEGs with survival significance. TMEscore, age, stage, grade, therapy outcome and histology are shown as patient annotations. Top legend, gray indicates missing value. (**E–G**) Forest plots illustrate the results of multivariate Cox proportional hazards model of clinical feature in all patients, CR patients and non-CR patients respectively.

groups. Among a total of 13 differentially mutated genes between two groups ($P < 0.05$; Supplementary Figure 5C), eight genes such as BRCA1, OR2G6, SHROOM3 showed a higher mutation frequency in the high TMEscore group. The other five genes, such as CHD6, TECTA, had a higher mutation frequency in low TMEscore group. Subsequently, we calculated the TMB and found that TMEscore could distinguish TMB and related to patients' OS ($P = 0.018$) (Supplementary Figure 5D).

Expression of immune-checkpoint between TMEscore groups

In addition, we found that TMEscore could predict the response of ICIs and could provide a basis for subsequent immunotherapy. By comparing the expression of immune checkpoints (CD80, CD86, and PDCD1) and stromal and immune scores computed by ESTIMATE between different groups, we found that they were highly expressed in high TMEscore group in TCGA and GEO (Figure 5A–5C, 5F–5H, 5I–5K, 5L–5Q). IPS was introduced to evaluate the patients' responses to ICI treatment because of the information

on ICI treatment was not available in TCGA and GEO datasets. The IPS values (IPS-CTLA-4_pos and IPS-PD-1/PD-L1/PD-L2_pos) as the alternative of the ovarian cancer patients' responses to anti-CTLA-4 and anti-PD-1/PD-L1 treatment were increased in the high TMEscore group (Figure 5D, 5E). It's likely that the patients in the high TMEscore group have a better immune microenvironment and respond better to ICIs.

DISCUSSION

The researchers have made various attempts to prolong the survival time of ovarian cancer patients by combining targeted therapy and chemotherapy [12]. Increased understanding of TME has shifted from a tumor cell centered view of cancer progression to the concept of a complex TME that supports tumor growth and metastatic dissemination. TME significantly influences therapeutic response and clinical outcomes for patients [4, 16]. In this study, TMEscore with the information of TME, developed and validated with more than 2,000 ovarian cancer patients, was found to be an independent prognostic biomarker and could improve treatment decisions in ovarian cancer.
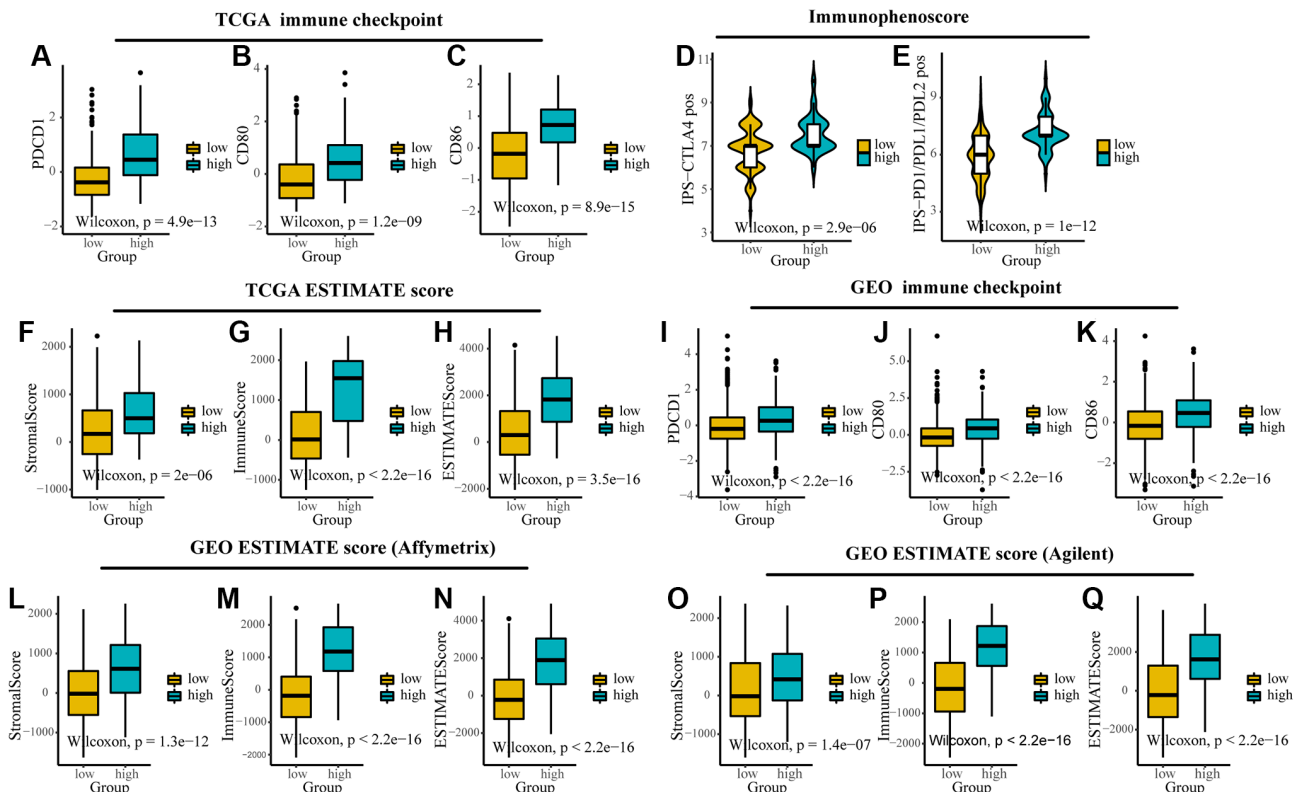

Figure 5. The expression of immune checkpoints and immune-related scores between different TMEscore groups in TCGA and GEO. (**A–C**) Expression of immune checkpoints (PDCD1, CD80 and CD86) between different groups in TCGA. (**D**, **E**) The relative probabilities to respond to anti-CTLA-4 and anti-PD-1/PD-L1 treatment in the low and high TMEscore group. (**F–I**) Expression of stromal score, immune score and ESTIMATE score between different groups in TCGA. (**J–L**) Expression of immune checkpoints (PDCD1, CD80 and CD86) between different groups in GEO. (**M–Q**) Expression of stromal score, immune score and ESTIMATE score between different groups in different platforms in GEO. The lines in the boxes represented median value.

Three distinct subtypes of ovarian cancer were found based on TME. According to previous studies, CD8 T cells were generally associated with a longer OS in tumors, while the presence of M0, M2 macrophages favoring tumor growth and spreading was associated with poor outcomes [17–19] (Figure 1). Through the enrichment of DEGs between subtypes of TME, we found that gene-cluster A was related to immune functions such as, chemokine, TNF and other cytokines act through cell surface receptors (Figure 2E). Cytokines are associated with expanding and reactivating effector NK and T lymphocytes, promoting lymphocytes tumor infiltration and persistence in TME [20]. And several biological processes correlated with immune regulation were found, including T-cell activation and leukocyte migration [21, 22]. While the pathways in gene-cluster B were usually related to cell growth, migration and proliferation (Figure 2F). Studies demonstrated that PI3K/AKT/mTOR pathway, one of the most important signaling pathways for therapeutic intervention in ovarian cancer, has been reported as the frequently altered signaling pathway in ovarian cancer [23]. And EGFR, VEGFR and BRAF targets in MAPK signaling pathway has been extensively studied for promising cancer treatment [24].

Because of characterizing and quantifying above cluster of genes, TMEscore is more biologically meaningful. At present, the predictive marker constructed by gene expression may be affected by some factors such as different platform expression and complexity of biological networks in a large number of genes. PCA is a mathematical algorithm that reduces the dimensionality of the data while retaining most of the variation in the data set. In this study, PCA was used to reduce further the dimension of the gene clusters with biological information.

Recently, numerous successful clinical trials have demonstrated that ICI treatment opens new cancer immunology avenues. However, only a small proportion of patients benefit from this therapy [25]. Therefore, we aim to find the biomarker for predicting therapeutic effect. As a significant component of the TME, immune infiltrates have been proven to mediate the tumor progression and immunotherapy responses [26]. For example, higher immune infiltration is associated with improved disease-specific survival under different treatment conditions of muscle-invasive bladder cancer. In contrast, higher stromal infiltration is associated with unfavorable disease-specific survival [27]. Meanwhile, high expression of PD-L1 and tumor-infiltrating lymphocytes are more likely to respond to ICI in advanced melanoma [28]. This study found that TMEscore had great potential in predicting ICI response. IPS values, checkpoints expression and

immune score were highly expressed in high TMEscore group. Resultantly, the high TMEscore group was more likely to benefit from immunotherapy and TMEscore could be used as a biomarker to immunotherapies and individualize treatment strategies.

Furthermore, we found that BRCA1 had more mutations in the high TMEscore group and speculated that high TMEscore patients might be a beneficiary population of PARP inhibitors combined with immunotherapy. As a key gene in gynecological tumors, some studies concluded that patients with BRCA mutations have a better response to platinum therapy than those without BRCA mutations [29]. And HR (Homologous Recombination) deficient ovarian cancer may be more sensitive to PD-1/PD-L1 inhibitors, and BRCA 1 and 2 mutations may leading HR deficient [30]. Olaparib, a PARP inhibition, had been approved by EMA and FDA for ovarian cancer patients with conditions such as BRCA mutations [31]. Therefore, we believe that the PARP inhibition treatment may be feasible in the high TMEscore group. Currently, the experimental results show that the combination of Olaparib and PD-1 can further improve the clinical outcome of ovarian cancer [32]. Besides, emerging clinical data suggest additive activity between PARP inhibition and PD-1/PD-L1 blockade, regardless of BRCA1/2-mutation status and HR deficiency [33]. These results collectively illustrate that high TMEscore group could benefit from a combination of ICIs and PARP inhibition treatment, and TMEscore is a promising therapeutic predictor in ovarian cancer.

Despite the comprehensive analysis of TMEscore, there are still some limitations in this study. Firstly, the method of PCA dimension reduction of multiple genes may be inferior to the predictive factor constructed by gene expression in biological interpretation. Secondly, incomplete clinical information in GEO has decreased the statistical power in multivariable Cox regression analysis. Third, the results are based only on the public databases, so further experiments are needed to verify its biological function.

In conclusion, TMEscore was a promising prognostic marker to explore the therapeutic direction of ovarian cancer as well as possible drugs that have substantial benefit for patients. Further biological validation is needed for this exploratory study.

MATERIALS AND METHODS

Datasets and preprocessing

We systematically searched for ovarian cancer gene-expression datasets that were publicly available and

Table 1. Demographic and clinic features descriptions for ovarian cancer patients in TCGA and GEO.

Characteristics	GSE13876	GSE14764	GSE17260	GSE19829	GSE23554	GSE26193	GSE26712	GSE30161	GSE32062	GSE32063	GSE49997	GSE51088	GSE53963	GSE63885	GSE73614	TCGA
Number of samples	415	80	110	70	28	107	185	58	260	40	194	116	160	75	107	373
Median survival time	24	55	54	46	53.3	36.6	46.0	51.0	60	54	NA	42.5	35.3	37.5	97	45.2
(month) (95% CI)	(21,30)	(51, NA)	(49, NA)	(36,72)	(37.4, NA)	(29.9, 54.7)	(38.9, 58.0)	(32.8, 75.0)	(50,80)	(40, NA)	(44, NA)	(36.0, 57.0)	(26.0, 45.5)	(29.9, 43.9)	(73, 156)	(41.6, 49.5)
Number of Death (%)	302 (72.8)	21 (26.3)	46 (41.8)	40 (57.1)	14 (50.0)	76 (71.0)	129 (69.7)	36 (62.1)	121 (46.5)	22 (55.0)	57 (29.4)	91 (78.4)	139 (86.9)	66 (88.0)	58 (54.2)	230 (61.7)
Median PFS/DFS/	–	–	19	19	–	21.3	–	13.4	19	21	19	–	–	–	–	18.4
RECUR time (95% CI)			(15, 26)	(15, 34)		(18.3, 24.5)		(10.9, 17.0)	(18, 23)	(15, 43)	(15, 21)					(16.8, 20.9)
Number of PFS/DFS/RECUR (%)																
YES	–	–	76 (69.1)	41 (58.6)	–	80 (74.8)	–	48 (82.8)	193 (74.2)	27 (67.5)	124 (63.9)	–	–	–	–	244 (65.4)
NO	–	–	34 (30.9)	14 (20.0)	–	27 (25.2)	–	6 (10.3)	67 (25.8)	13 (32.5)	70 (36.1)	–	–	–	–	129 (34.6)
unknown	–	–	–	15 (21.4)	–	–	–	4 (6.9)	–	–	–	–	–	–	–	–
Age (years)	57.95 ± 12.29	–	–	60.50 ± 11.22	–	–	–	62.57 ± 10.61	–	–	57.66 ± 11.82	60.65 ± 12.07	63.61 ± 11.41	–	61.31 ± 10.89	59.60 ± 11.37
<55	160 (38.6)	–	–	25 (35.7)	–	–	–	15 (25.9)	–	–	77 (39.7)	37 (31.9)	36 (22.5)	–	32 (29.9)	131 (35.1)
≥55	255 (61.4)	–	–	45 (64.3)	–	–	–	43 (74.1)	–	–	117 (60.3)	79 (68.1)	124 (77.5)	–	75 (70.1)	242 (64.9)
Histology type (%)	–	–	–	–	–	–	–	–	–	–	–	–	–	–	–	–
serous	–	68 (85)	–	65 (92.9)	–	79 (73.8)	–	47 (81.0)	–	–	171 (88.1)	90 (77.6)	–	70 (93.3)	4 (3.7)	373 (100.0)
others	–	12 (15)	–	5 (7.1)	–	28 (26.2)	–	9 (15.5)	–	–	23 (11.9)	26 (22.4)	–	5 (6.7)	103 (96.3)	0 (0)
unknown	–	–	–	–	–	–	–	2 (3.4)	–	–	–	–	–	–	–	–
FIGO stage (%)	–	–	–	–	–	–	–	–	–	–	–	–	–	–	–	–
I & II	–	9 (11.2)	0 (0)	3 (4.3)	–	31 (29.0)	–	0 (0)	0 (0)	0 (0)	9 (4.6)	21 (18.1)	7 (4.4)	2 (2.7)	48 (44.9)	22 (5.9)
III & IV	–	71 (88.8)	110 (100.0)	67 (95.7)	–	76 (71.0)	–	58 (100.0)	260 (100.0)	40 (100.0)	185 (95.4)	95 (81.9)	153 (95.6)	73 (97.3)	59 (55.1)	348 (93.3)
unknown	–	–	–	–	–	–	–	–	–	–	–	–	–	–	–	3 (0.8)
Grade (%)	–	–	–	–	–	–	–	–	–	–	–	–	–	–	–	–
G1 & G2 (Mod & Well)	–	26 (32.5)	67 (60.9)	10 (14.3)	10 (35.7)	40 (37.4)	–	21 (36.2)	131 (50.4)	23 (57.5)	50 (25.8)	19 (16.4)	3 (1.9)	9 (12.0)	29 (27.1)	43 (11.5)
G3 & G4 (Poor)	–	54 (67.5)	43 (39.1)	60 (85.7)	18 (64.3)	67 (62.6)	–	33 (56.9)	129 (49.6)	17 (42.5)	143 (73.7)	97 (83.6)	157 (98.1)	66 (88.0)	78 (72.9)	320 (85.8)
unknown	–	–	–	–	–	–	–	4 (6.9)	–	–	1 (0.5)	–	–	–	–	10 (2.7)
Therapy outcome	–	–	–	–	–	–	–	–	–	–	–	–	–	–	–	–
CR	–	–	–	–	18 (64.3)	–	–	32 (55.2)	–	–	–	–	–	50 (66.7)	–	196 (70.5)
non-CR	–	–	–	–	10 (35.7)	–	–	23 (39.7)	–	–	–	–	–	25 (33.3)	–	82 (29.5)
unknown	–	–	–	–	–	–	–	3 (5.2)	–	–	–	–	–	–	–	–

reported with full clinical annotations in GEO (https://www.ncbi.nlm.nih.gov/geo/) [34] and TCGA (https://xenabrowser.net/datapages/) [35]. Patients without survival information were removed from further evaluation. Meanwhile, patients initially recorded as recurrent in TCGA were also removed. Finally, we gathered sixteen ovarian cancer cohorts from GEO and TCGA for this study (Table 1) and summarized the detailed medication information (Supplementary Table 4). RNA-seq and microarray gene expression data were preprocessed separately. For microarray data from Affymetrix®, we downloaded the raw "CEL" files and processed them using the RMA algorithm for performing background adjustment, quantile normalization etc., in the "Affy" package. The normalized matrix files were downloaded directly for microarray data from other platforms. The raw data provided by GSE13876 was processed by log2 transformation and quantile standardization. For TCGA dataset, RNA sequencing data (FPKM value) of gene expression were downloaded and transformed into transcripts per kilobase million (TPM). Probesets that mapped to more than one gene symbol were summarized by their median expression value. Genes with a missing value of more than 50% were deleted, and the remaining missing values were imputed with KNN imputation approaches. Batch effects from non-biological technical biases were corrected using the "ComBat" algorithm of "sva" package [36]. The somatic mutation data (SNPs and small INDELs) was downloaded from TCGA database (MuTect2 Variant Aggregation and Masking) (https://xenabrowser.net/datapages/) [35]. Finally, a total of 2,378 ovarian cancer patients with 6,008 genes were included in this study.

Inference of infiltrating cells in TME and phenotype-associated genes

To explore TME and TME-related phenotypes in ovarian cancer, a deconvolution algorithm, CIBERSORT, was utilized to accurately quantify the proportions of immune cells in TME within a complex gene expression

mixture (https://cibersort.stanford.edu/index.php). It distinguishes 22 human hematopoietic cell phenotypes (LM22), including seven T-cell types, naïve and memory B cells, plasma cells, natural killer (NK) cells and myeloid subsets. Next, nonnegative matrix factorization (NMF), an unsupervised algorithm, was used to find the cluster of TME-infiltrating cells. The differentially expressed genes (DEGs) associated with the TME phenotype were determined by both linear models and nonlinear models for RNA-seq data. The linear model was performed using the "limma" package with adjusted $P < 0.05$ [37]. Random forest classification algorithm was used as the non-linear model for DEGs identification.

TME gene signature

To predict the prognosis of ovarian cancer, TMEscore was constructed by quantifying the TME characterization of individual tumor. A three-step method was used to establish TMEscore. First, consensus clustering algorithm was applied to define the cluster of DEGs, as DEGs may be related to different biological functions in TME. Then, the "clusterProfiler" package [38] was adopted to annotate gene patterns of Kyoto Encyclopedia of Genes and Genomes (KEGG) pathway and Gene Ontology (GO) enrichment [39, 40]. Furthermore, univariate Cox regression was performed to identify prognostic genes for each gene (transformed into a z-score) in the cluster. Moreover, PCA was used to construct TME relevant gene signature. Principal component 1 was selected to act as signature scores. Finally, TMEscore was calculated similar to GGI method [41]:

$$TMEscore = \sum PC1_i - \sum PC1_j$$

where i is the signature score of clusters whose Cox coefficient is negative, and j is the expression of genes whose Cox coefficient is positive. This method has the advantage of focusing the score on the set with the largest block of well correlated (or anticorrelated) genes in the set, while down-weighting contributions from genes that do not track with other set members.

A prognostic nomogram with TMEscore

To determine the prognostic significance of TMEscore in ovarian cancer, log-rank test and multivariate Cox regression model were fitted in this analysis. Meanwhile, to eliminate the influence of chemotherapy outcome on prognosis, we performed a chemotherapy outcome-stratified analysis of all patients with therapeutic information. A nomogram is considered an important component of decision-making in modern medicine. It could generate an individual possibility of a clinical event by integrating various prognostic and determinant variables, providing assistance for personalized medicine [42]. Therefore, we constructed a nomogram with age, stage, grade, chemotherapy outcome and TMEscore to predict the probability of 3- and 5-year OS. The calibration curve was drawn to evaluate the nomogram prediction possibilities against the observed rates.

Identification of gene mutations

Some mutant-specific drugs are emerging as the preferred first-line therapy for cancers [43]. We combined the mutation information with TMEscore to explore appropriate treatment of different TMEscore groups and improve the treatment strategy. The "Maftools" package was used to present the mutation landscape, identify the differentially genes mutations between groups and calculate tumor mutational burden (TMB).

Predicting the patients' response to ICI

The Cancer Immunome Atlas (https://tcia.at/) analyzed the immune landscapes and antigenomes of 20 solid tumors and were quantified by Immunophenoscore [44] (IPS, a superior immune response molecular marker). The IPS value, ranged from 0 to 10, was positively correlated to tumor immunogenicity and has been verified that IPS could predict the patients' response to immune checkpoints inhibitors (ICIs treatment). The immune checkpoint expressions between different TMEscore groups were observed intuitively by drawing box and violin diagrams. The fraction of stromal and immune cells was inferred using the ESTIMATE method [45].

Statistical analysis

Continuous variables were summarized as mean ± SD and categorized variables were described by frequency (n) and proportion (%). Wilcoxon rank-sum test or Kruskal-Wallis test were used to compare two or three groups of quantitative variables. For comparisons of qualitative variables, statistical significance was estimated by Fisher's exact tests. The cutoff value was calculated based on the correlation between the patients' survival and the TMEscore in TCGA using "surv_cutpoint" function with the "survminer" package. The "surv_cutpoint" function, which repeatedly tested all potential thresholds in order for the maximum rank statistic, was applied to dichotomize TMEscore. Kaplan–Meier (K–M) curves were generated to illustrate the prognostic analysis and log-rank tests were utilized to identify significance of differences. The

concordance index (C-index) was calculated to investigate performance of the TMEscore prognostic model. The nomogram and calibration curve were generated with "rms" package. The heatmap was produced by R package "ComplexHeatmap". We list all R packages used in this paper in Supplementary Table 5. All statistical *P* values were two sides, with *P* < 0.05 as statistically significance. All data processing was done in R 4.0.2 software.

Abbreviations

TME: The tumor microenvironment; PD-1: programmed cell death-1; PD-L1: Programmed death-ligand 1; OS: Overall survival; PFS: Progression-free survival; ORR: Overall response rate; LM22: 22 human hematopoietic cell phenotypes; NK: Natural killer; NMF: Nonnegative matrix factorization; KEGG: Kyoto Encyclopedia of Genes and Genomes; C-index: Concordance index.

AUTHOR CONTRIBUTIONS

Kang Li and Yan Hou designed the study; Zhenyi Xu and Jiali Song wrote the manuscript; Zhenyi Xu, Jiali Song, Jia He, and Zhiwei Rong downloaded and analyzed the data; Lei Cao and Wenjie Zhang prepared all the figures and tables. All authors reviewed and approved the final manuscript.

CONFLICTS OF INTEREST

The authors declare no conflicts of interest related to this study.

FUNDING

REFERENCES

1. Whiteside TL. The tumor microenvironment and its role in promoting tumor growth. Oncogene. 2008; 27:5904–12.
   https://doi.org/10.1038/onc.2008.271
   PMID:18836471

2. Hinshaw DC, Shevde LA. The Tumor Microenvironment Innately Modulates Cancer Progression. Cancer Res. 2019; 79:4557–66.
   https://doi.org/10.1158/0008-5472.CAN-18-3962
   PMID:31350295

3. Hui L, Chen Y. Tumor microenvironment: Sanctuary of the devil. Cancer Lett. 2015; 368:7–13.
   https://doi.org/10.1016/j.canlet.2015.07.039
   PMID:26276713

4. Pitt JM, Marabelle A, Eggermont A, Soria JC, Kroemer G, Zitvogel L. Targeting the tumor microenvironment: removing obstruction to anticancer immune responses and immunotherapy. Ann Oncol. 2016; 27:1482–92.
   https://doi.org/10.1093/annonc/mdw168
   PMID:27069014

5. Constantinidou A, Alifieris C, Trafalis DT. Targeting Programmed Cell Death -1 (PD-1) and Ligand (PD-L1): A new era in cancer active immunotherapy. Pharmacol Ther. 2019; 194:84–106.
   https://doi.org/10.1016/j.pharmthera.2018.09.008
   PMID:30268773

6. Postow MA, Callahan MK, Wolchok JD. Immune Checkpoint Blockade in Cancer Therapy. J Clin Oncol. 2015; 33:1974–82.
   https://doi.org/10.1200/JCO.2014.59.4358
   PMID:25605845

7. Hamanishi J, Mandai M, Ikeda T, Minami M, Kawaguchi A, Murayama T, Kanai M, Mori Y, Matsumoto S, Chikuma S, Matsumura N, Abiko K, Baba T, et al. Safety and Antitumor Activity of Anti-PD-1 Antibody, Nivolumab, in Patients With Platinum-Resistant Ovarian Cancer. J Clin Oncol. 2015; 33:4015–22.
   https://doi.org/10.1200/JCO.2015.62.3397
   PMID:26351349

8. Satoh T, Kang YK, Chao Y, Ryu MH, Kato K, Cheol Chung H, Chen JS, Muro K, Ki Kang W, Yeh KH, Yoshikawa T, Oh SC, Bai LY, et al. Exploratory subgroup analysis of patients with prior trastuzumab use in the ATTRACTION-2 trial: a randomized phase III clinical trial investigating the efficacy and safety of nivolumab in patients with advanced gastric/gastroesophageal junction cancer. Gastric Cancer. 2020; 23:143–53.
   https://doi.org/10.1007/s10120-019-00970-8
   PMID:31087200

9. Siegel RL, Miller KD, Jemal A. Cancer statistics, 2019. CA Cancer J Clin. 2019; 69:7–34.
   https://doi.org/10.3322/caac.21551
   PMID:30620402

10. Torre LA, Trabert B, DeSantis CE, Miller KD, Samimi G, Runowicz CD, Gaudet MM, Jemal A, Siegel RL. Ovarian cancer statistics, 2018. CA Cancer J Clin. 2018; 68:284–96.
    https://doi.org/10.3322/caac.21456
    PMID:29809280

11. Odunsi K. Immunotherapy in ovarian cancer. Ann Oncol. 2017; 28:viii1–7.
    https://doi.org/10.1093/annonc/mdx444
    PMID:29232467

12. Kuroki L, Guntupalli SR. Treatment of epithelial ovarian cancer. BMJ. 2020; 371:m3773.
https://doi.org/10.1136/bmj.m3773
PMID:33168565

13. Liu JF, Herold C, Gray KP, Penson RT, Horowitz N, Konstantinopoulos PA, Castro CM, Hill SJ, Curtis J, Luo W, Matulonis UA, Cannistra SA, Dizon DS. Assessment of Combined Nivolumab and Bevacizumab in Relapsed Ovarian Cancer: A Phase 2 Clinical Trial. JAMA Oncol. 2019; 5:1731–8.
https://doi.org/10.1001/jamaoncol.2019.3343
PMID:31600397

14. Newman AM, Liu CL, Green MR, Gentles AJ, Feng W, Xu Y, Hoang CD, Diehn M, Alizadeh AA. Robust enumeration of cell subsets from tissue expression profiles. Nat Methods. 2015; 12:453–7.
https://doi.org/10.1038/nmeth.3337
PMID:25822800

15. Brunet JP, Tamayo P, Golub TR, Mesirov JP. Metagenes and molecular pattern discovery using matrix factorization. Proc Natl Acad Sci U S A. 2004; 101:4164–9.
https://doi.org/10.1073/pnas.0308531101
PMID:15016911

16. Wu T, Dai Y. Tumor microenvironment and therapeutic response. Cancer Lett. 2017; 387:61–8.
https://doi.org/10.1016/j.canlet.2016.01.043
PMID:26845449

17. Ali HR, Chlon L, Pharoah PD, Markowetz F, Caldas C. Patterns of Immune Infiltration in Breast Cancer and Their Clinical Implications: A Gene-Expression-Based Retrospective Study. PLoS Med. 2016; 13:e1002194.
https://doi.org/10.1371/journal.pmed.1002194
PMID:27959923

18. Becht E, Giraldo NA, Germain C, de Reyniès A, Laurent-Puig P, Zucman-Rossi J, Dieu-Nosjean MC, Sautès-Fridman C, Fridman WH. Immune Contexture, Immunoscore, and Malignant Cell Molecular Subgroups for Prognostic and Theranostic Classifications of Cancers. Adv Immunol. 2016; 130:95–190.
https://doi.org/10.1016/bs.ai.2015.12.002
PMID:26923001

19. Fridman WH, Pagès F, Sautès-Fridman C, Galon J. The immune contexture in human tumours: impact on clinical outcome. Nat Rev Cancer. 2012; 12:298–306.
https://doi.org/10.1038/nrc3245
PMID:22419253

20. Berraondo P, Sanmamed MF, Ochoa MC, Etxeberria I, Aznar MA, Pérez-Gracia JL, Rodríguez-Ruiz ME, Ponz-Sarvise M, Castañón E, Melero I. Cytokines in clinical cancer immunotherapy. Br J Cancer. 2019; 120:6–15.
https://doi.org/10.1038/s41416-018-0328-y
PMID:30413827

21. Diehl AD, Lee JA, Scheuermann RH, Blake JA. Ontology development for biological systems: immunology. Bioinformatics. 2007; 23:913–5.
https://doi.org/10.1093/bioinformatics/btm029
PMID:17267433

22. Lieber S, Reinartz S, Raifer H, Finkernagel F, Dreyer T, Bronger H, Jansen JM, Wagner U, Worzfeld T, Müller R, Huber M. Prognosis of ovarian cancer is associated with effector memory CD8$^+$ T cell accumulation in ascites, CXCL9 levels and activation-triggered signal transduction in T cells. Oncoimmunology. 2018; 7:e1424672.
https://doi.org/10.1080/2162402X.2018.1424672
PMID:29721385

23. Ediriweera MK, Tennekoon KH, Samarakoon SR. Role of the PI3K/AKT/mTOR signaling pathway in ovarian cancer: Biological and therapeutic significance. Semin Cancer Biol. 2019; 59:147–60.
https://doi.org/10.1016/j.semcancer.2019.05.012
PMID:31128298

24. Burotto M, Chiou VL, Lee JM, Kohn EC. The MAPK pathway across different malignancies: a new perspective. Cancer. 2014; 120:3446–56.
https://doi.org/10.1002/cncr.28864
PMID:24948110

25. Iwai Y, Hamanishi J, Chamoto K, Honjo T. Cancer immunotherapies targeting the PD-1 signaling pathway. J Biomed Sci. 2017; 24:26.
https://doi.org/10.1186/s12929-017-0329-9
PMID:28376884

26. Zhang Y, Zhang Z. The history and advances in cancer immunotherapy: understanding the characteristics of tumor-infiltrating immune cells and their therapeutic implications. Cell Mol Immunol. 2020; 17:807–21.
https://doi.org/10.1038/s41423-020-0488-6
PMID:32612154

27. Efstathiou JA, Mouw KW, Gibb EA, Liu Y, Wu CL, Drumm MR, da Costa JB, du Plessis M, Wang NQ, Davicioni E, Feng FY, Seiler R, Black PC, et al. Impact of Immune and Stromal Infiltration on Outcomes Following Bladder-Sparing Trimodality Therapy for Muscle-Invasive Bladder Cancer. Eur Urol. 2019; 76:59–68.
https://doi.org/10.1016/j.eururo.2019.01.011
PMID:30712971

28. Teng MW, Ngiow SF, Ribas A, Smyth MJ. Classifying Cancers Based on T-cell Infiltration and PD-L1. Cancer Res. 2015; 75:2139–45.
https://doi.org/10.1158/0008-5472.CAN-15-0255
PMID:25977340

29. Neff RT, Senter L, Salani R. *BRCA* mutation in ovarian cancer: testing, implications and treatment considerations. Ther Adv Med Oncol. 2017; 9:519–31.

https://doi.org/10.1177/1758834017714993
PMID:28794804

30. Ventriglia J, Paciolla I, Pisano C, Cecere SC, Di Napoli M, Tambaro R, Califano D, Losito S, Scognamiglio G, Setola SV, Arenare L, Pignata S, Della Pepa C. Immunotherapy in ovarian, endometrial and cervical cancer: State of the art and future perspectives. Cancer Treat Rev. 2017; 59:109–16.
https://doi.org/10.1016/j.ctrv.2017.07.008
PMID:28800469

31. George A, Kaye S, Banerjee S. Delivering widespread BRCA testing and PARP inhibition to patients with ovarian cancer. Nat Rev Clin Oncol. 2017; 14:284–96.
https://doi.org/10.1038/nrclinonc.2016.191
PMID:27958297

32. Ding L, Kim HJ, Wang Q, Kearns M, Jiang T, Ohlson CE, Li BB, Xie S, Liu JF, Stover EH, Howitt BE, Bronson RT, Lazo S, et al. PARP Inhibition Elicits STING-Dependent Antitumor Immunity in Brca1-Deficient Ovarian Cancer. Cell Rep. 2018; 25:2972–80.e5.
https://doi.org/10.1016/j.celrep.2018.11.054
PMID:30540933

33. Lee EK, Konstantinopoulos PA. Combined PARP and Immune Checkpoint Inhibition in Ovarian Cancer. Trends Cancer. 2019; 5:524–8.
https://doi.org/10.1016/j.trecan.2019.06.004
PMID:31474356

34. Barrett T, Wilhite SE, Ledoux P, Evangelista C, Kim IF, Tomashevsky M, Marshall KA, Phillippy KH, Sherman PM, Holko M, Yefanov A, Lee H, Zhang N, et al. NCBI GEO: archive for functional genomics data sets-- update. Nucleic Acids Res. 2013; 41:D991–5.
https://doi.org/10.1093/nar/gks1193
PMID:23193258

35. Goldman MJ, Craft B, Hastie M, Repečka K, McDade F, Kamath A, Banerjee A, Luo Y, Rogers D, Brooks AN, Zhu J, Haussler D. Visualizing and interpreting cancer genomics data via the Xena platform. Nat Biotechnol. 2020; 38:675–8.
https://doi.org/10.1038/s41587-020-0546-8
PMID:32444850

36. Leek JT, Johnson WE, Parker HS, Jaffe AE, Storey JD. The sva package for removing batch effects and other unwanted variation in high-throughput experiments. Bioinformatics. 2012; 28:882–3.
https://doi.org/10.1093/bioinformatics/bts034
PMID:22257669

37. Ritchie ME, Phipson B, Wu D, Hu Y, Law CW, Shi W, Smyth GK. limma powers differential expression analyses for RNA-sequencing and microarray studies. Nucleic Acids Res. 2015; 43:e47.
https://doi.org/10.1093/nar/gkv007
PMID:25605792

38. Yu G, Wang LG, Han Y, He QY. clusterProfiler: an R package for comparing biological themes among gene clusters. OMICS. 2012; 16:284–7.
https://doi.org/10.1089/omi.2011.0118
PMID:22455463

39. Ashburner M, Ball CA, Blake JA, Botstein D, Butler H, Cherry JM, Davis AP, Dolinski K, Dwight SS, Eppig JT, Harris MA, Hill DP, Issel-Tarver L, et al. Gene ontology: tool for the unification of biology. Nat Genet. 2000; 25:25–9.
https://doi.org/10.1038/75556
PMID:10802651

40. Kanehisa M, Goto S. KEGG: kyoto encyclopedia of genes and genomes. Nucleic Acids Res. 2000; 28:27–30.
https://doi.org/10.1093/nar/28.1.27
PMID:10592173

41. Sotiriou C, Wirapati P, Loi S, Harris A, Fox S, Smeds J, Nordgren H, Farmer P, Praz V, Haibe-Kains B, Desmedt C, Larsimont D, Cardoso F, et al. Gene expression profiling in breast cancer: understanding the molecular basis of histologic grade to improve prognosis. J Natl Cancer Inst. 2006; 98:262–72.
https://doi.org/10.1093/jnci/djj052
PMID:16478745

42. Balachandran VP, Gonen M, Smith JJ, DeMatteo RP. Nomograms in oncology: more than meets the eye. Lancet Oncol. 2015; 16:e173–80.
https://doi.org/10.1016/S1470-2045(14)71116-7
PMID:25846097

43. Mok TS, Wu YL, Thongprasert S, Yang CH, Chu DT, Saijo N, Sunpaweravong P, Han B, Margono B, Ichinose Y, Nishiwaki Y, Ohe Y, Yang JJ, et al. Gefitinib or carboplatin-paclitaxel in pulmonary adenocarcinoma. N Engl J Med. 2009; 361:947–57.
https://doi.org/10.1056/NEJMoa0810699
PMID:19692680

44. Charoentong P, Finotello F, Angelova M, Mayer C, Efremova M, Rieder D, Hackl H, Trajanoski Z. Pan-cancer Immunogenomic Analyses Reveal Genotype-Immunophenotype Relationships and Predictors of Response to Checkpoint Blockade. Cell Rep. 2017; 18:248–62.
https://doi.org/10.1016/j.celrep.2016.12.019
PMID:28052254

45. Yoshihara K, Shahmoradgoli M, Martínez E, Vegesna R, Kim H, Torres-Garcia W, Treviño V, Shen H, Laird PW, Levine DA, Carter SL, Getz G, Stemke-Hale K, et al. Inferring tumour purity and stromal and immune cell admixture from expression data. Nat Commun. 2013; 4:2612.
https://doi.org/10.1038/ncomms3612
PMID:24113773
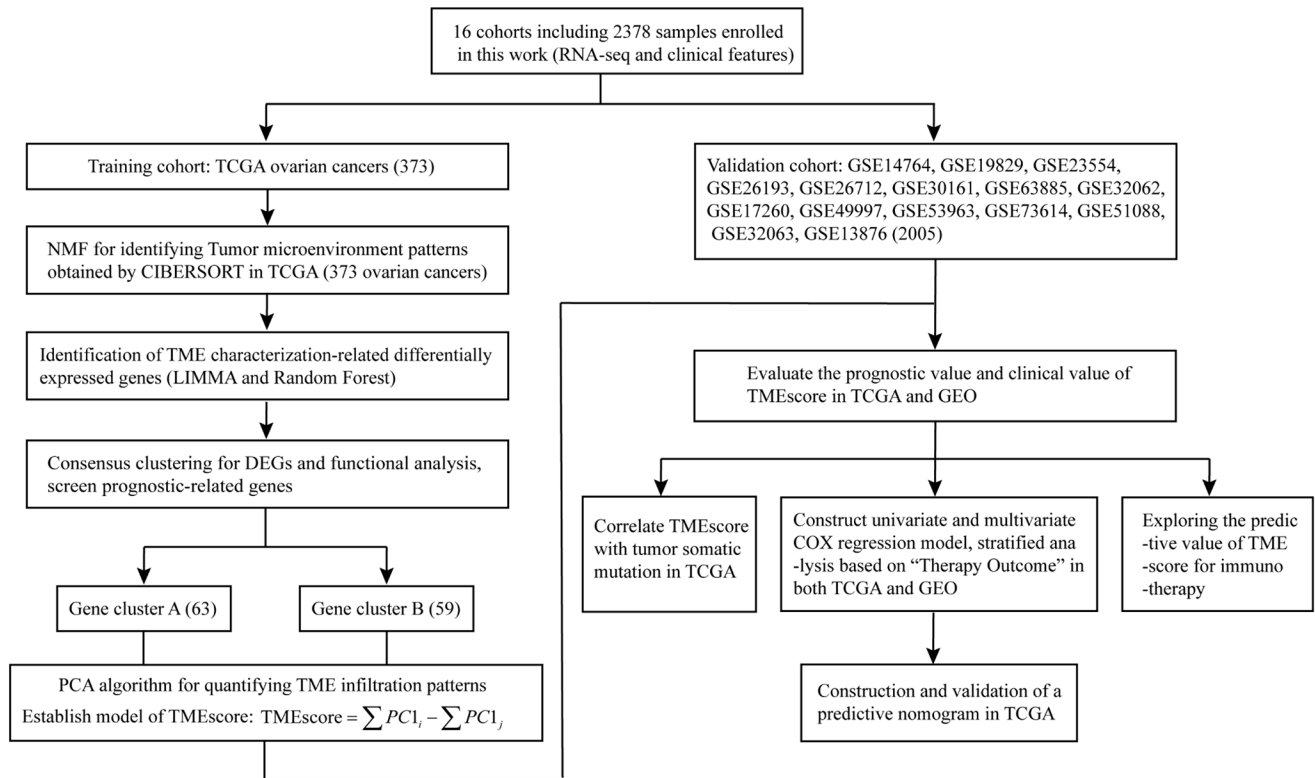
**Supplementary Figure 1. Overview of study design.**
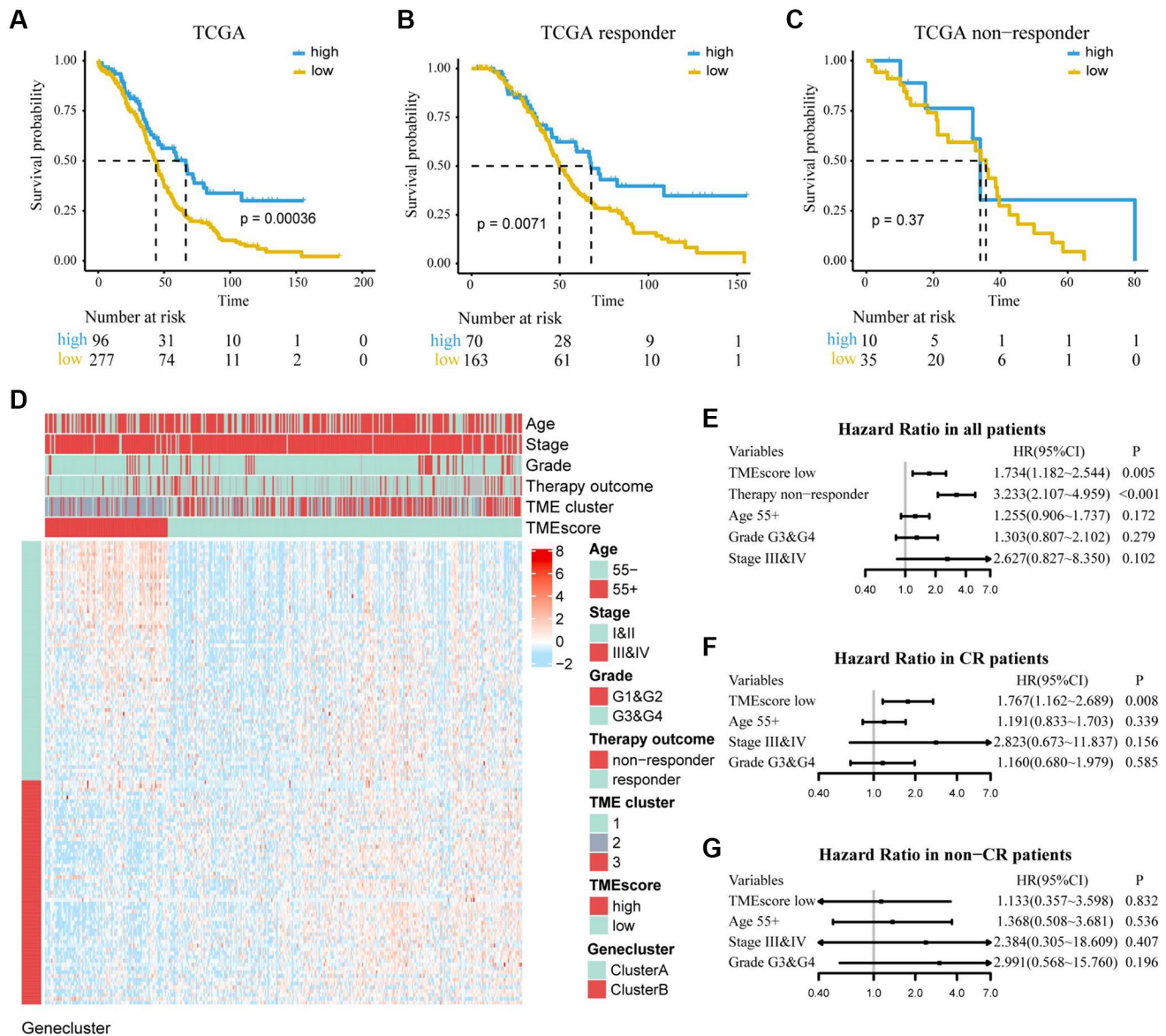
Supplementary Figure 2. Sensitivity analysis determine the prognostic group of 373 ovarian cancer patients based on TMEscore in TCGA and evaluate the predictive ability. (**A**) K–M curve for OS of different TMEscore groups (log-rank test, *P* < 0.001). (**B**, **C**) According to chemotherapy outcome-stratified analysis (278 ovarian cancer patients), K–M curves in patients with responders (CR and PR) or non-responders (non-CR and non-PR) in different TMEscore group (log-rank test, *P* = 0.007; log-rank test, *P* = 0.37). (**D**) Expression profile of DEGs with survival significance. TMEscore, age, stage, grade, therapy outcome and TME cluster are shown as patient annotations. GeneClass is shown as gene annotations. Top legend, gray indicates missing value. (**E**–**G**) Forest plots illustrate the results of multivariate Cox proportional hazards model of clinical feature in all patients, responders and non-responders respectively.
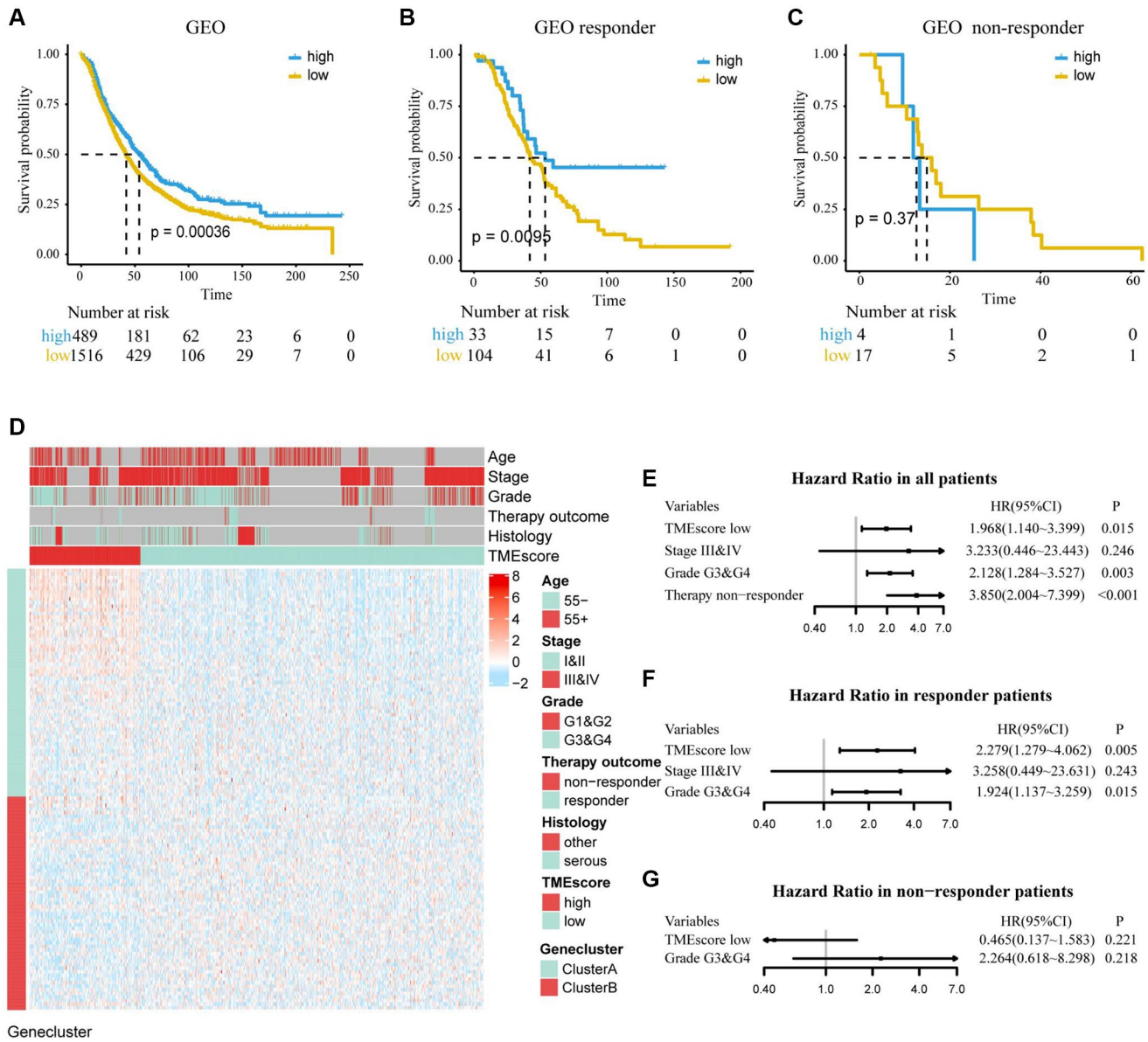
Supplementary Figure 3. Sensitivity analysis determine the prognostic group of 2005 ovarian cancer patients based on TMEscore in GEO and evaluate the predictive ability. (**A**) K–M curve for OS of different TMEscore groups (log-rank test, *P* < 0.001). (**B**, **C**) According to chemotherapy outcome-stratified analysis (158 ovarian cancer patients), K–M curves in patients with responders (CR and PR) or non-responders (non-CR and non-PR) in different TMEscore group (log-rank test, *P* = 0.0095; log-rank test, *P* = 0.37). (**D**) Expression profile of DEGs with survival significance. TMEscore, age, stage, grade, therapy outcome and histology are shown as patient annotations. Top legend, gray indicates missing value. (**E**–**G**) Forest plots illustrate the results of multivariate Cox proportional hazards model of clinical feature in all patients, responders and non-responders respectively.
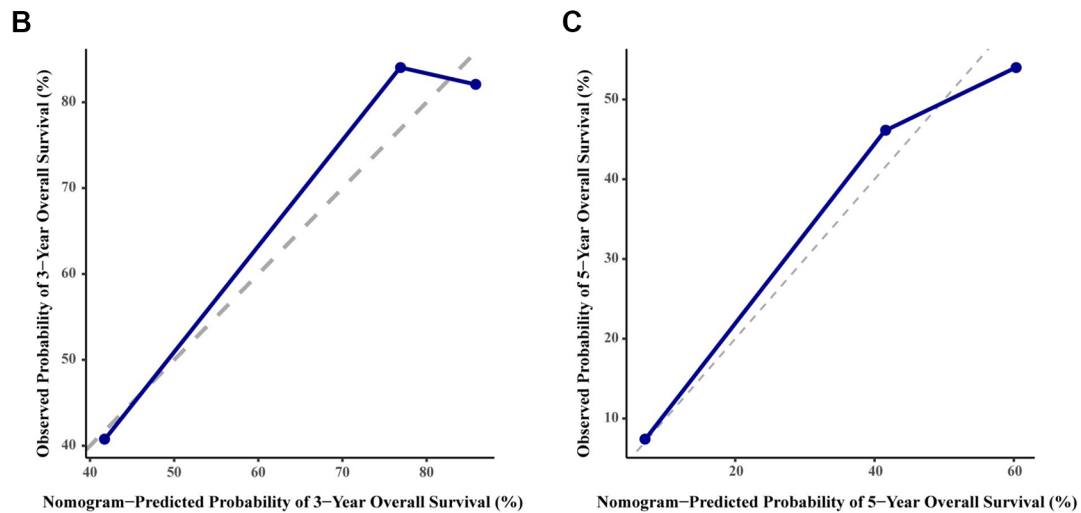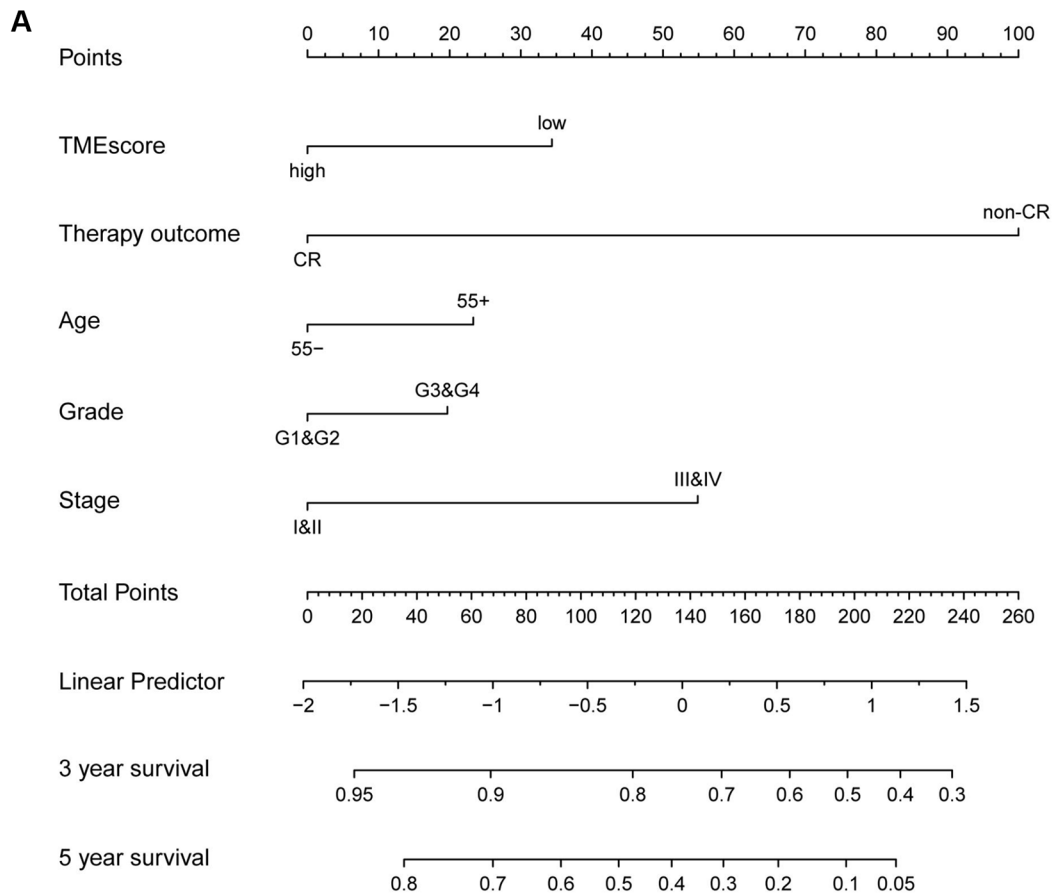
Supplementary Figure 4. Nomogram of clinical features in TCGA. (**A**) Nomogram for predicting the probability at 3- or 5-year OS based on clinical features. (**B**, **C**) Calibration curves of the nomogram for predicting the probability of OS at 3-, and 5-years.
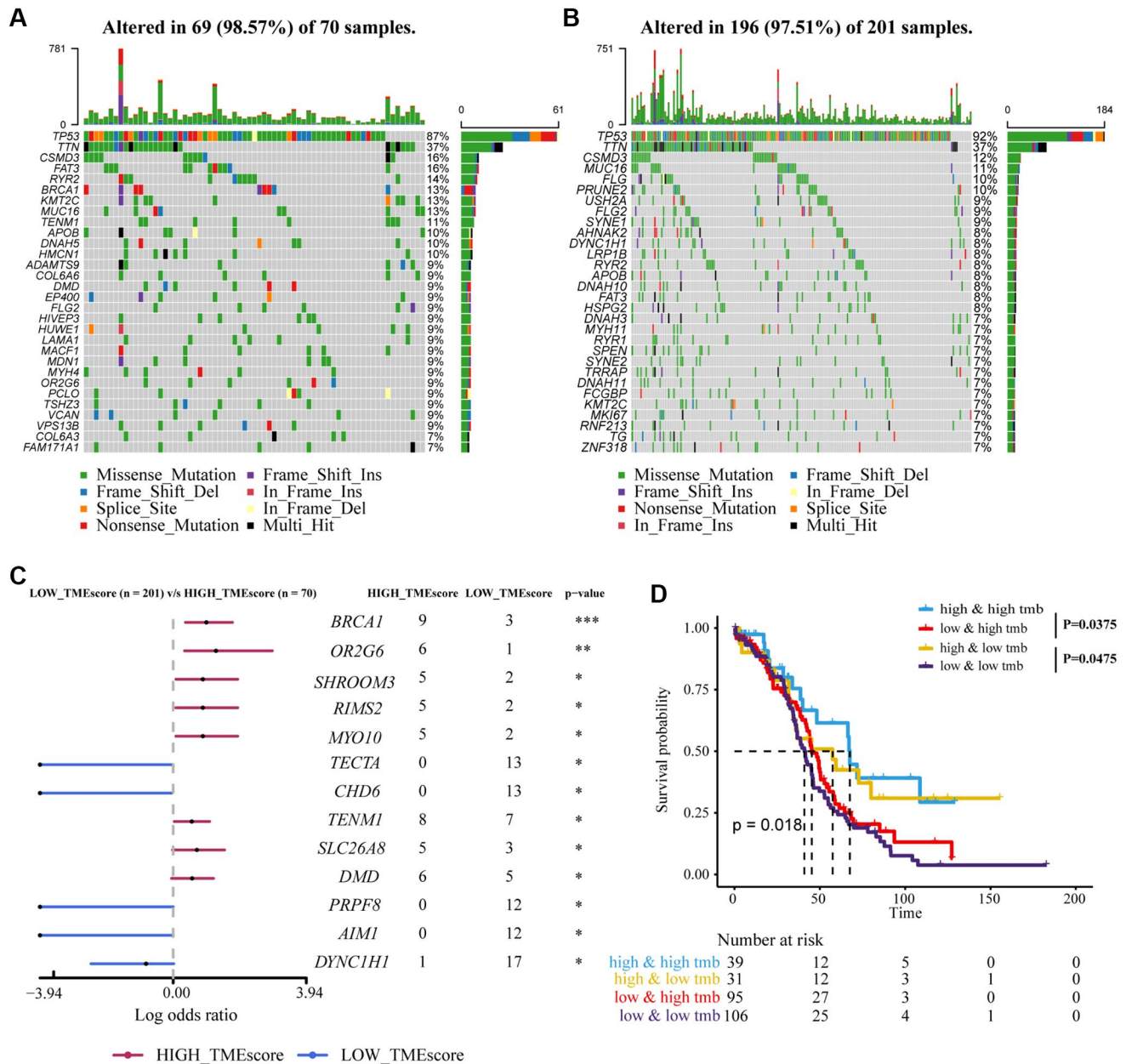
Supplementary Figure 5. The mutation landscape between high and low TMEscore groups. (**A**, **B**) Mutation profile of high and low TMEscore groups. (**C**) Comparing differential mutated genes between TMEscore groups by Fisher's exact tests. The asterisks represented the statistical *P* value. (*$P < 0.05$; **$P < 0.01$; ***$P < 0.001$). (**D**) K–M curves for patients in TCGA cohort stratified by both receipt of tumor mutational burden (TMB, cutoff value was calculated by median) and TMEscore (log-rank test, $P = 0.018$).

Supplementary Tables

Please browse Full Text version to see the data of Supplementary Tables 1–3.

Supplementary Table 1. The proportions of tumor microenvironment cells in 373 ovarian cancer patients.

Supplementary Table 2. Pathway enrichment analyses (KEGG) of genes cluster A and B.

Supplementary Table 3. Gene Ontology (GO) enrichment of genes cluster A and B (TOP 50).

Supplementary Table 4. The detailed medication information in different datasets.

The detailed medication information TCGA

Drug	Number of medication	Overall (333)
Platinum (Carboplatin, Cisplatin, Cisplatin+Gemcitabine, Oxaliplatin, Paclitaxel+Carboplatin, Topotecan+Carboplatin) (%)	0	8 (2.4)
	1	315 (94.6)
	2	10 (3.0)
Paclitaxel (%)	0	35 (10.5)
	1	267 (80.2)
	2	31 (9.3)
Others (%)	0	281 (84.4)
	1	51 (15.3)
	2	1 (0.3)
Unknown (%)	0	331 (99.4)
	1	2 (0.6)

The detailed medication information GSE30161

Drug	Overall (58)
Carboplatin	2 (3.4)
Carboplatin/Cytoxan	1 (1.7)
Carboplatin/Taxol	49 (84.5)
Cisplatin/Cytoxan	1 (1.7)
Cisplatin/Taxol	5 (8.6)

The detailed medication information GSE63885

Drug	Overall (75)
Platinum/Cyclophosphamide	34 (45.3)
Taxane/Platinum	41 (54.7)

The detailed medication information GSE23554

Drug	Overall (28)
Cisplatin	28 (100.0)

Supplementary Table 5. Summary of R package.

R package	Function
Affy	The package contains functions for Affymetrix GeneChip data analysis
clusterProfiler	Statistical analysis and visualization of functional profiles for genes and gene clusters
ComplexHeatmap	The package was used to visualize heatmap
ConsensusClusterPlus	The package was used to perform unsupervised clustering
estimate	The fraction of stromal and immune cells was calculated by estimate package
forestplot	The package was used to visualize forest plot
ggplot2	The package was used for data visualization
limma	Limma was used to identify the differentially expressed genes
maftools	The MAF files was analysed by maftools
NMF	Provides a framework to perform Non-negative Matrix Factorization
org.Hs.eg.db	Genome wide annotation for Human, primarily based on mapping using Entrez Gene identifiers.
psych	Principal component analysis was performed with psych
randomForest	The package was used to identify the differentially expressed genes
rms	The nomogram and calibration curve were generated with rms package
survival	Survival analysis was performed by survival package
survminer	Determine the optimal cutpoint for continuous variables and visualize the survival curves
sva	Removing batch effects in high-throughput experiment
tableone	The baseline patient characteristics was described by tableone